Verifiably exact solution of the electronic Schrödinger equation on quantum devices

Scott E. Smart⬤ and David A. Mazziotti⬤*

Department of Chemistry and The James Franck Institute, The University of Chicago, Chicago, Illinois 60637, USA

Quantum computers have the potential for a significant speedup of molecular computations. However, existing algorithms have limitations; quantum phase estimation (QPE) is intractable on current hardware while variational quantum eigensolvers (VQE) are dependent upon approximate wave functions without guaranteed convergence. In this paper we present an algorithm that yields verifiably exact solutions of the many-electron Schrödinger equation. Rather than solve the Schrödinger equation directly, we solve its contraction over all electrons except two, known as the contracted Schrödinger equation (CSE). The CSE generates a wave-function *Ansatz*, constructed from an iterative product of nonunitary two-body transformations, whose energy gradient with respect to the two-body operator of the current iteration vanishes if and only if the CSE is satisfied. Because the CSE implies the Schrödinger equation, the two-electron *Ansatz* provides a verifiably exact *Ansatz* for solving the many-electron Schrödinger equation. The exactness property contrasts with that of *Ansätze* built from the product of unitary two-body transformations where the gradient—the residual of the anti-Hermitian part of the CSE (ACSE)—can vanish without implying a solution of the Schrödinger equation. We demonstrate the algorithm on both simulators and noisy quantum computers with H_2 dissociation and the rectangle-to-square transition in H_4.

I. INTRODUCTION

The wave function of a many-particle quantum system scales exponentially with the number of particles, and hence, it can be computationally advantageous to compute the energy and other one- and two-particle expectation values [i.e., the two-particle reduced density matrix (2-RDM)] without computing the wave function [1–6]. A natural equation for the determining the 2-RDM is obtained from contracting the matrix formulation of the Schrödinger equation over all particles save two, generating the contracted Schrödinger equation (CSE) [7–9]. The CSE has the significant, nontrivial property that a wave function satisfies the CSE if and only if it satisfies the Schrödinger equation [7,10]. In classical electronic structure algorithms, however, the CSE is indeterminate in the solution of the 2-RDM because it depends upon not only the 2-RDM but also the higher three- and four-particle RDMs (3- and 4-RDMs). While the indeterminacy of the equation can be removed by reconstructing higher RDMs in terms of the 2-RDM [11–14], the reconstruction introduces an approximation, which limits applications of the CSE from being exact.

In this paper we show that many-particle quantum systems can be solved on a noiseless quantum computer from the solution of the CSE for the 2-RDM. The reconstruction of higher RDMs in the CSE, required on classical computers, can be avoided on a quantum computer through a combination of state preparations and 2-RDM measurements. The CSE extends a family of algorithms, known as contracted quantum eigensolvers (CQE), in which the residual of a contracted

eigenvalue equation is solved on a quantum computer to generate a solution of the original eigenvalue problem [15–19]. The solution of the CSE generates a series of nonunitary, two-body transformations that provide an exact *Ansatz* for the wave function [20–22]. The wave-function *Ansatz* is exact in that the gradient of the energy with respect to the two-body operator of the current iteration vanishes if and only if the CSE, and hence the many-electron Schrödinger equation, are satisfied. In all previous versions of the CQE, the anti-Hermitian part of CSE (ACSE) [23–30], which keeps the two-body exponential transformations unitary, was used as the contracted equation. However, the ACSE, unlike the CSE, does not necessarily satisfy the Schrödinger equation upon its solution, which can in principle lead to problems where the ACSE is satisfied away from a eigenstate.

In contrast to many variational quantum eigensolvers (VQE) [31–33] which use approximate wave-function *Ansätze*, the proposed CQE for solving the CSE converges in the absence of noise to a solution of the CSE that corresponds to an exact many-particle solution of the Schrödinger equation. The CSE *Ansatz* for the wave function is more scalable than the conventional coupled cluster *Ansatz* because it is exact with only two-body transformations [20] while the coupled cluster *Ansatz* requires 2- to N-particle excitations [20,34]. Each two-body transformation in the product has been shown to correspond to an order of perturbation theory which guarantees rapid convergence in the vicinity of the solution [21]. Additionally, the CQE approach performs the optimization based on the residual of the contracted equation, and hence does not require any VQE-based subroutines, seen in adaptive or iterative based approaches [22,35–37]. In this work we provide examples of the exactness of the CSE-based CQE, and additionally apply the CQE to molecular H_2 on a

---

*damazz@uchicago.edu

superconducting quantum device, as well as noiseless simulations of the rectangle-to-square transition in H_4 with quantum simulators.

II. THEORY

We discuss the CSE in Sec. II A, the exact *Ansatz* for the wave function that arises from the CSE in Sec. II B, and the quantum algorithm for solving the CSE in Sec. II C.

A. Contracted Schrödinger equation

For many-particle quantum systems with at most pairwise interactions, consider the contraction of the matrix formulation of the Schrödinger equation to generate the CSE [7–10,20],

$$\langle \Psi | \hat{a}_i^\dagger \hat{a}_j^\dagger \hat{a}_l \hat{a}_k (\hat{H} - E) | \Psi \rangle = 0, \tag{1}$$

where $\hat{H}$ is the Hamiltonian operator, $|\Psi\rangle$ is the wave function of a given state, E is the energy of the state, and $a_i^\dagger (a_i)$ is the second-quantized creation (annihilation) operator for a particle in orbital i. For convenience we assume that the wave function and the Hamiltonian are real. The CSE has the following important property: if the Hamiltonian has at most pairwise interactions, a wave function satisfies the CSE if and only if it satisfies the Schrödinger equation. The Schrödinger equation clearly implies the CSE, but the opposite direction is provable from showing that the CSE implies the energy variance which in turn implies the Schrödinger equation [7,10].

The CSE [7–10,20] can be expressed as the sum of its Hermitian and its anti-Hermitian components

$$^2R^{ij;kl} = \tfrac{1}{2}(^2S^{ij;kl} + {}^2A^{ij;kl}) = 0, \tag{2}$$

where

$$^2S^{ij;kl} = \langle \Psi | \{ \hat{a}_i^\dagger \hat{a}_j^\dagger \hat{a}_l \hat{a}_k, (\hat{H} - E) \} | \Psi \rangle \tag{3}$$

and

$$^2A^{ij;kl} = \langle \Psi | [\hat{a}_i^\dagger \hat{a}_j^\dagger \hat{a}_l \hat{a}_k, \hat{H}] | \Psi \rangle \tag{4}$$

are the Hermitian CSE (HCSE) and the ACSE [23–30], respectively. Previous CQE algorithms [15–19] have been based on a solution of the ACSE. The advantage of using the ACSE rather than the CSE as the basis for CQE is that the iterative solution of the ACSE implies a wave-function *Ansatz* based on the product of unitary two-body transformations [15]. The disadvantage of using the ACSE, however, is that the solution of the ACSE does not theoretically imply the solution of the many-electron Schrödinger equation [20,24], even though practically it has been shown in noiseless quantum simulations to converge to the solution from exact diagonalization (full configuration interaction) for a variety of molecular systems [15–19]. The goal of the present work is to develop the theory and algorithm for a CQE based on the CSE in which the solution of the CSE by nonunitary two-body transformations implies the solution of the many-electron Schrödinger equation.

B. Exact wave-function *Ansatz*

The CSE, it has been shown previously [20,21], implies that the exact many-body wave function $|\Psi\rangle$ has a minimal parametrization in which it is expressed as a product of M two-body exponential transformations applied to a mean-field reference wave function $|\Psi_0\rangle$ as follows:

$$\left| \Psi_{n+1}^{\text{CSE}} \right\rangle = e^{\epsilon \hat{R}_n} \left| \Psi_n^{\text{CSE}} \right\rangle, \tag{5}$$

where $\hat{R}_n$ for each $n = 1, 2, ..., M$ is a general two-body operator

$$\hat{R}_n = \sum_{ijkl} {}^2R_n^{ij;kl} \hat{a}_i^\dagger \hat{a}_j^\dagger \hat{a}_l \hat{a}_k, \tag{6}$$

in which $^2R_n^{ij;kl}$ is a two-body matrix element. Importantly, differentiating the energy with respect to the matrix elements of ^2R_n yields the residual of the CSE,

$$^2R_n^{ij;kl} = \lim_{\epsilon \to 0} \frac{1}{2\epsilon} \frac{d}{dR_n^{kl;ij}} \langle \Psi_n | e^{\epsilon \hat{R}_n^\dagger} (\hat{H} - E) e^{\epsilon \hat{R}_n} | \Psi_n \rangle \tag{7}$$

$$= \langle \Psi_n | \hat{a}_i^\dagger \hat{a}_j^\dagger \hat{a}_l \hat{a}_k (\hat{H} - E) | \Psi_n \rangle + O(\epsilon). \tag{8}$$

Upon convergence of the energy at the final iteration M, the gradient of the energy with respect to the parameters $^2R_M^{ij;kl}$ vanishes, implying the satisfaction of the CSE. Consequently, all local minima of this *Ansatz* for the wave function correspond to solutions of the CSE and hence, solutions of the Schrödinger equation, proving that this wave-function *Ansatz* is exact [20,21].

We can also use the Hermitian $\hat{S}_n$ and anti-Hermitian $\hat{A}_n$ parts of the CSE residual to define HCSE and ACSE wave-function *Ansätze* [20,21,24]:

$$\left| \Psi_{n+1}^{\text{HCSE}} \right\rangle = e^{\epsilon \hat{S}_n} \left| \Psi_n^{\text{HCSE}} \right\rangle \tag{9}$$

and

$$\left| \Psi_{n+1}^{\text{ACSE}} \right\rangle = e^{\epsilon \hat{A}_n} \left| \Psi_n^{\text{ACSE}} \right\rangle, \tag{10}$$

which upon convergence imply the HCSE and ACSE, respectively. Because the Hamiltonian is Hermitian, the solution of the HCSE like that of the CSE also implies the energy variance and hence, solution of the Schrödinger equation [20,21]. Even though the HCSE is only part of the CSE, its solution implies that of the entire CSE, and therefore, like the CSE *Ansatz*, the HCSE *Ansatz* in Eq. (9) is also an exact *Ansatz* whose critical points correspond to stationary-state solutions of the Schrödinger equation. In contrast, the ACSE *Ansatz* in Eq. (10) only converges to a solution of the ACSE that is not guaranteed to imply the Schrödinger equation. We can define a family of exact wave-function *Ansätze* in which we alternate between HCSE and ACSE updates in Eqs. (9) and (10), respectively. If we apply both HCSE and ACSE updates at each iteration, we have the following form for the wave function:

$$\left| \Psi_{n+1}^{\text{HCSE-ACSE}} \right\rangle = e^{\epsilon \hat{S}_n} e^{\epsilon \hat{A}_n} \left| \Psi_n^{\text{HCSE-ACSE}} \right\rangle, \tag{11}$$

whose stationarity also implies the CSE. Because the HCSE part requires the application of a nonunitary transformation, it can also be applied less frequently; in fact, the HCSE can even be applied just once at the end of any electronic wave-function *Ansatz* to verify the exactness of the solution.

Because each two-body transformation in the product in Eq. (5), Eq. (9), or Eq. (11) can be selected to correspond to an order of perturbation theory in the wave function [21], the

solution can converge rapidly with the number of iterations in the vicinity of the solution. Importantly, the number of iterations depends on the quality of the initial guess. Moreover, because the method is size extensive, the total number of iterations is independent of size when the system consists of Q independent fragments with Q tending to infinity. As shown for the ACSE, the rate of convergence of the CSE also depends on whether a first-order or second-order optimization is performed; see Ref. [18] for more details.

C. CQE algorithm

On classical computers, to avoid the exponential-scaling cost of computing and storing the wave function, the CSE or ACSE is reexpressed in terms of RDMs [7–9,23,24,26–30,38], with the higher-order RDMs being approximated as functionals of the 2-RDM [11]. This RDM-based approach based on the ACSE has been accurately applied to treating strong correlated molecular electronic behavior with both ground and excited states including photoexcitations [26,30] and conical intersections [27,28]. On a quantum computer, however, the wave function in Eq. (5) can be prepared and the 2-RDM can be measured without reconstructing the higher RDMs , allowing us to solve the CSE for, in principle, exact simulations of many-particle quantum systems.

1. Preparation of the Ansatz

To solve the CSE on quantum computers, we can prepare the wave function using the *Ansatz* in either Eq. (5), Eq. (9), or Eq. (11). We select Eq. (11) because it allows us to interweave ACSE updates, which we have previously developed [15–19], with HCSE updates, which we develop and implement below. At each iteration the wave function in Eq. (11) is normalized by dividing by the square root of the normalization factor $N = \langle \Psi_{n+1} | \Psi_{n+1} \rangle$. The sums within both $\hat{S}_n$ and $\hat{A}_n$ are implemented via Trotterization, although when ϵ is small, the error is negligible. The step size must be selected to provide improvement towards the solution of the CSE; while it cannot be too large due to the Trotterization approximation, it also cannot be too small due to the noise present on the quantum device. In this sense, it is used as a proxy for assessing the error of implementing a target operator [e.g., $\exp(\epsilon \hat{S}_n)$] on the device. In practice, the step size can be a fixed learning rate (small) or a parameter that is optimized to minimize the energy in a line search— see Algorithm 1. For more details on specific optimization methods, see Ref. [18]. To implement the exponential operator $e^{\epsilon \hat{S}_n}$, we develop a dilation approach, adapted from the quantum simulation of nonunitary dynamics [39], in which we embed the nonunitary transformation in a unitary transformation. While not discussed in detail here, other approaches to nonunitary dynamics such as the least-squares-based imaginary time-evolution technique [40] can also be adapted.

Consider an operator $V[\hat{S}_n]$

$$V[\hat{S}_n] = \begin{bmatrix} 1 & \epsilon \hat{S}_n \\ -\epsilon \hat{S}_n & 1 \end{bmatrix}, \qquad (12)$$

which acts to produce a state:

$$V[\hat{S}_n][|\Psi\rangle \quad |\Psi\rangle]^T = [e^{\epsilon \hat{S}_n}|\Psi\rangle \quad e^{-\epsilon \hat{S}_n}|\Psi\rangle] + O(\epsilon^2). \quad (13)$$

Algorithm 1. CQE for solving the contracted Schrödinger equation by nonunitary two-body exponentials transformations. Given initial state $|\Psi\rangle$, an optimization procedure $\mathcal{O}$ [which inputs an energy function, wave function, and residual (gradient) and outputs the energy and search direction], and a nonunitary implementation $\mathcal{T}$, the algorithm generates a solution of the CSE including the energy E within an error threshold γ.

Inputs: $\Psi_0, \mathcal{O}, H, \mathcal{T}$
Output: Ψ_M, E_M.
  0a: Set $n \leftarrow 0$
  0b: Define $E[\Psi, \hat{R}] = \langle \Psi | e^{\mathcal{T}[\hat{R}^\dagger]} \hat{H} e^{\mathcal{T}[\hat{R}]} | \Psi \rangle / \langle \Psi | e^{\mathcal{T}[\hat{R}^\dagger + \hat{R}]} | \Psi \rangle$
  0c: Calculate $\hat{R}_0$
  While $||^2 \hat{R}_n|| > \gamma$:
    1: $E_{n+1}, \epsilon_n \hat{R}_n = \mathcal{O}(E[\Psi_n, \hat{R}_n], \Psi_n, \hat{R}_n)$
    2: Update $|\Psi_{n+1}\rangle = \mathcal{T}[\epsilon_n \hat{R}_n] | \Psi_n \rangle$
    3: $n \leftarrow n + 1$

This can be realized in a quantum algorithm by expanding the state space with a single ancilla, and then applying a Pauli gadget with the Pauli Y matrix:

$$V[\hat{S}_n] = e^{i \delta \hat{Y}_a \otimes \hat{S}_n}. \qquad (14)$$

This method works well for small steps, and is similar to techniques for approximating nonunitary time evolution [39]. The remaining problem relates to subsequent evolutions, which is not generally addressed. To proceed exactly, we can either append another ancilla [41] or perform a projective measurement to select the particular ancilla state. Both of these approaches, however, decrease the success probability roughly by half, having exponentially decreasing success rates [42]. Instead, we directly implement the next operator without an ancilla or projective measurement, which can be shown to generate the target operator to first order. After several steps (on the order of $\frac{1}{\epsilon}$) the first-order approximation will fail, and hence, we use a loose Wolfe condition [43] to determine when to perform a reset or dilation onto another ancilla. The proposed method still leads to an exponentially decreasing success probability, but with a much slower decay than in the previous methods. In theory, performing a type of amplitude amplification [44,45], which can specifically target the propagated operators of interest, could further mitigate this effect, although for near-term results this is likely not feasible. Details comparing effective strategies for implementing this operator will be compared in future work.

2. Measurement of the CSE residual

To obtain the residuals, we can express the residual of the CSE as the average of the HCSE and ACSE residuals that require the 4-RDM and 3-RDM, respectively [see Eq. (2)]. We again turn to an ancilla-based expansion of the wave function, where we can perturb the wave function and recover information on the contracted equation to some controlled approximation. While there likely are ways to recover the ACSE and HCSE residuals simultaneously, in a circuit-based measurement these are similar to the real and imaginary tomography of a 2-RDM, which naturally can be separated. Hence, we simply separate the ACSE and HCSE residuals into two auxiliary state methods. This method of obtaining
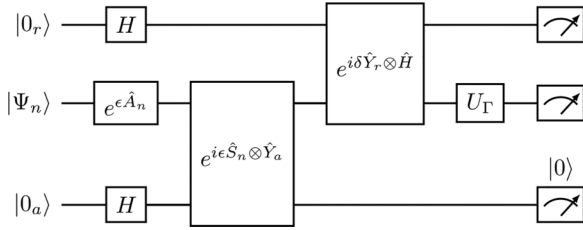
FIG. 1. Method of implementing the CSE *Ansatz* for the contracted quantum eigensolver. At a given iteration n, we implement the Trotterizations of the exponential of $\hat{A}_n$, and then the nonunitary exponential of $\hat{S}_n$ using a single ancilla qubit. Measurement of a 2-RDM element is represented by Γ_k. Note that H denotes the Hadamard gate while $\hat{H}$ denotes the Hamiltonian. Information on the residuals can be obtained using a conditioned time evolution operator, as well as the traditional time evolution operator.

the ACSE to second-order accuracy in δ has been documented previously [15], and we can envision a method of obtaining the HCSE to a similar accuracy as follows.

Let W be a unitary acting on a single ancilla coupled with $|\Psi\rangle$ to produce an auxiliary state $|\Upsilon\rangle$:

$$\hat{W} = \begin{bmatrix} 1 - \frac{\delta^2}{2}\hat{H}^2 & +\delta\hat{H} \\ -\delta\hat{H} & 1 - \frac{\delta^2}{2}\hat{H}^2 \end{bmatrix}, \quad (15)$$

and

$$|\Upsilon\rangle = \frac{1}{\sqrt{2}}\hat{W}[|\Psi\rangle \quad |\Psi\rangle]^T. \quad (16)$$

Performing the following 2-RDM-related measurement:

$$\hat{M}_{kl}^{ij} = \begin{bmatrix} \hat{a}_i^\dagger \hat{a}_j^\dagger \hat{a}_l \hat{a}_k & 0 \\ 0 & -\hat{a}_i^\dagger \hat{a}_j^\dagger \hat{a}_l \hat{a}_k \end{bmatrix}, \quad (17)$$

yields the following residuals:

$$\frac{1}{\delta}\langle\Upsilon|\hat{M}|\Upsilon\rangle = {}^2S^{ij;kl} + O(\delta^2). \quad (18)$$

On a quantum computer, we can readily perform this operation where $\hat{W}$ corresponds to a Pauli-conditioned time evolution operator and $\hat{M}_{kl}^{ij}$ to a Pauli-conditioned 2-RDM measurement:

$$\hat{W} = \exp\left(i\delta Y_a \otimes \hat{H}\right), \quad \hat{M}_{kl}^{ij} = Z_a \otimes \hat{a}_i^\dagger \hat{a}_j^\dagger \hat{a}_l \hat{a}_k, \quad (19)$$

in which Y_a, Z_a are the Pauli Y and Z gates acting on the ancilla a, which we have prepared by applying the Hadamard transform to the ancilla. Because the Pauli terms are present in every operator, these Pauli conditioned operators possess the same scaling as their original operators. In practice, care must be taken with the relative precisions such that δ is significantly larger than the sampling errors. It may be possible to alleviate these concerns [44,45] by using amplitude estimation or possibly expansions of derivative-based estimates for operators [46]. Figure 1 shows the implementation of the *Ansatz* for a particular iteration.

III. RESULTS

We consider three applications: (i) a pairing spin model, (ii) the dissociation of rectangular H_4, and (iii) the dissociation of
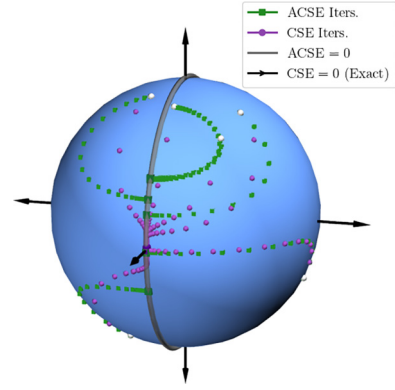

FIG. 2. Trajectories for the ACSE and CSE on the unit sphere, generated by the iterations in the algorithms from several initial guesses for a three-state system separated by sequential double excitations (i.e., the ground state and second excited state are separated by quadruple excitations). The unit sphere directly represents coordinates corresponding to amplitudes of c_0, c_1, and c_2. The axes along the gray line correspond to $\pm|0\rangle$ and $\pm|2\rangle$, and the perpendicular axes, the $|1\rangle$ states. States which are in the span of $|0\rangle$ and $|2\rangle$ satisfy the ACSE, but not necessarily the CSE.

H_2 on a noisy quantum device. The pairing spin model with two pairs of electrons, whose details are given in Appendix A, has three independent degrees of freedom corresponding to the excitation of zero, one, or two pairs that can be mapped to the unit sphere. Using a variety of initial guesses, we compute the ground-state energy on a noiseless simulator by minimizing the residuals of the ACSE and CSE, respectively. Figure 2 shows the solution trajectories on the unit sphere, generated by the iterations in the algorithms, for the ACSE and CSE for each of the initial guesses. The solutions of the four-electron Schrödinger equation and the CSE are shown by the black arrows with one hidden behind the sphere. Note that the six black arrows on the sphere denote the three solutions of the CSE represented twice through a global phase of ±1. While the solutions of the CSE are discrete, the ACSE has additional solutions in the form of a continuous family of solutions denoted by the gray circle. The ACSE iterations, shown by the green squares, converge for many initial guesses to spurious solutions lying on the gray circle where the ACSE's residual vanishes. In contrast, the two-electron CSE iterations, shown by the pink circles, correctly converge for each of the initial guesses to the unique ground state of the four-electron Schrödinger equation. Solution by the ACSE would require a fourth-order excitation *Ansatz*. These results, which are consistent with Ref. [20], highlight the importance of the CSE rather than the ACSE as the stationary condition for a CQE.

Figure 3 shows the performance of three CQE methods—CSE, ACSE, and HCSE—on noiseless simulations in the stretching of rectangular H_4 along one of its sides. The energy surface possesses a discontinuity at the square configuration that is difficult to capture with single-reference methods [34,47]. With all methods we are able to obtain the full configuration interaction solution at different dissociation lengths, including the discontinuity with its multireference correlation. In Fig. 3(c) we can also see a close relation between the (squared) norm of the residuals and the energy variance. While the CSE and HCSE residuals linearly
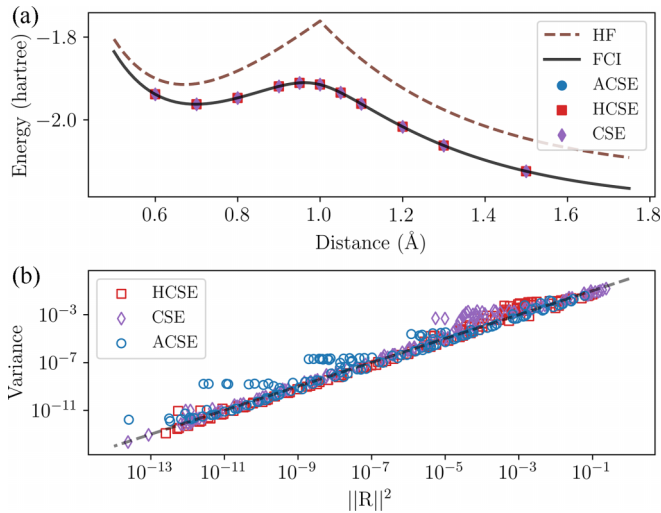
FIG. 3. Simulations of rectangular H_4 dissociation (with pairs kept at 1 Å) with a noise-free CQE: (a) energy dissociation curves and (b) comparison of CSE, HCSE, and ACSE residual norms and energy variances under several points in trajectories taken from (a).

follow the variance, the ACSE residual encounters temporary plateaus where it becomes disproportionately small relative to the variance, reflecting that unlike the case with the CSE and HCSE, the solution of the ACSE does not rigorously imply the solution of the Schrödinger equation, which is equivalent to the vanishing of the energy variance. Note that an upper bound on the variance in relation to the norms can be derived via the Cauchy-Schwarz inequality.

Finally, using the IBM QUANTUM EXPERIENCE, we simulate without error mitigation the dissociation of H_2 using the CSE. The simulation requires two qubits—one for the symmetry-tapered wave function and one for the nonunitary dilation. The target wave function is represented by a single qubit using symmetry tapering. Figure 4 shows that like the
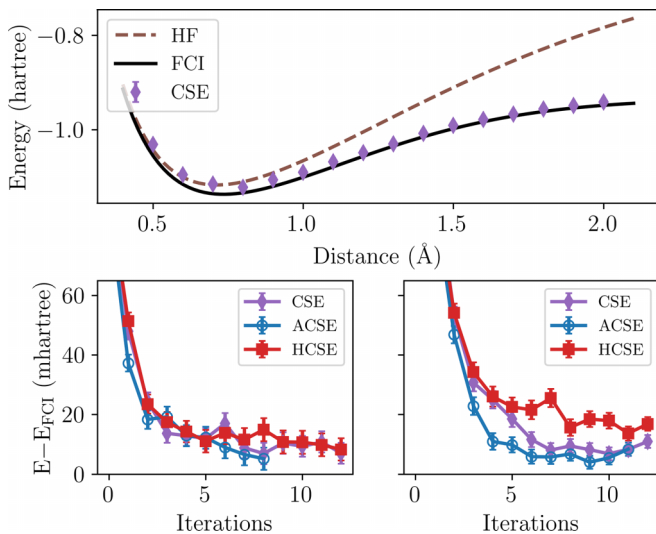

FIG. 4. Quantum computations on "ibm_lagos" of the dissociation of H_2 by the CSE, ACSE, and HCSE, as well as classical computations by Hartree-Fock and full configuration interaction.

ACSE, the CSE recovers correlation energy across the dissociation surface, with the accuracy limited only by sampling and noise-related errors. The differences in implementation here on noisy devices favors the ACSE, which relative to the CSE requires fewer multiqubit gates in a more compact *Ansatz*.

IV. DISCUSSION AND CONCLUSIONS

Many-particle quantum systems, we have shown, can in principle be solved from an exact solution of the CSE on quantum devices. The solution of the CSE is particularly attractive because it has the following important property: a wave function satisfies the CSE if and only if it satisfies the Schrödinger equation. Thus, the CSE provides a natural *Ansatz* for preparing the wave function, as well as a functional criterion for the successful convergence of the wave function. The CSE *Ansatz* has additional costs associated with its nonunitary propagation. As these can be mitigated in principle, or strictly limited (i.e., through the number of ancilla qubits), the CSE provides a flexible nonvariational approach for preparing the wave function without sacrificing exactness relative to the variational solution of the many-electron Schrödinger equation.

Previously, we have shown that the anti-Hermitian part of the CSE, known as the ACSE, can be solved on quantum devices [15]. While the ACSE *Ansatz* for the wave function has generally been observed to converge to the result from exact diagonalization (i.e., full configuration interaction) [18,24], only the CSE has a mathematical guarantee that its wave function solutions have a one-to-one mapping with the solutions of the Schrödinger equation [20,21]. As discussed in this paper, unlike the ACSE, optimization of the CSE on quantum devices requires the performance of nonunitary transformations. Because the ACSE is a subset of the CSE, the performance of nonunitary transformations that aim to satisfy the CSE can be interwoven with unitary transformations that aim to satisfy the ACSE. Moreover, the balance of unitary and nonunitary transformations can be controlled to optimize both accuracy and convergence on noisy intermediate-scale or fault-tolerant quantum devices, possibly aided through compression of two-body operators [48–50]. Additionally, the CSE can be invoked at the end of a CQE based on the ACSE or a VQE calculation to refine or verify convergence to an exact stationary point of the Schrödinger equation.

The solution of the CSE can be viewed as solving the many-particle problem on quantum devices based on an integration or contraction of the many-particle state, which in the context of the ACSE has been called a CQE. In contrast to the VQE [31,33] which generally has an approximate wave function *Ansatz* and relies upon variational improvement, the CQE based on the CSE has a scalable wave function *Ansatz* that by definition converges to the exact solution of the Schrödinger equation. Furthermore, unlike adaptive VQE [36], the CQE does not require variational reoptimization of all parameters at each iteration and is guaranteed to be exact when its energy gradient vanishes. Finally, the CSE-based CQE provides a framework for exploring nonunitary transformations in the quantum simulation of electronic structure. The combination of these unique features and potential advantages shows that the exact solution of the CSE on quantum devices provides an

important step forward for the quantum simulation of many-particle systems on intermediate-term and future quantum computers.

ACKNOWLEDGMENTS

APPENDIX A: THREE-SITE MODEL

The paired spin model, used in Fig. 2, describes a three-state system of sequential pair excitations, where the potential-free eigenstates are separated by double excitations, and the ground-to-second excited state requires a quadruple excitation. Denoting a pair population by 1, we can map this to the following states:

$$|0\rangle = |1010\rangle \tag{A1}$$

$$|1\rangle = |1001\rangle \tag{A2}$$

$$|2\rangle = |0110\rangle \tag{A3}$$

$$|3\rangle = |0101\rangle. \tag{A4}$$

Under a symmetric potential states $|1\rangle$ and $|2\rangle$ are degenerate, with the proper eigenstate being the positive linear combination of the two. Thus, we can map the three states, $|0\rangle$, $\frac{1}{\sqrt{2}}(|1\rangle + |2\rangle)$, and $|3\rangle$, to the unit sphere. Importantly, $|0\rangle \leftrightarrow |1\rangle$ and $|1\rangle \leftrightarrow |2\rangle$ are mediated through a single pair excitation (i.e., a double excitation), whereas the $|0\rangle \leftrightarrow |2\rangle$ transition requires two pair excitations (i.e., a four-electron term). This situation also can occur between combinations of high- and low-spin states, which are not coupled through two-electron Hamiltonians [51].

APPENDIX B: COMPUTATIONAL DETAILS

Results in Figs. 3 and 4 were performed using the HQCA (v22.9) [52] set of tools, which utilizes QISKIT (v0.29.0) [53], IBM QUANTUM [54], and PYSCF (v1.7.6) [55] for interfacing with quantum simulators and obtaining electron integrals for circuit-based simulations. All calculations used minimal basis sets (STO-3G). For Fig. 4, 16 000 shots for circuit measurements were used for the CSE and HCSE and 8000 for the ACSE, and $\mathbb{Z}_2$ symmetries were applied in order to reduce the Hamiltonian to a single qubit.

[1] *Advances in Chemical Physics*, edited by D. A. Mazziotti (John Wiley & Sons, Hoboken, 2007), Vol. 134, p. 574.

[2] A. Coleman and V. Yukalov, *Reduced Density Matrices: Coulson's Challenge* (Springer, Berlin, Heidelberg, 2000).

[3] *Many-Electron Densities and Reduced Density Matrices*, edited by J. Cioslowski, Mathematical and Computational Chemistry (Springer, Boston, 2000), Vol. 91, pp. 399–404.

[4] D. A. Mazziotti, Two-electron reduced density matrix as the basic variable in many-electron quantum chemistry and physics, Chem. Rev. **112**, 244 (2012).

[5] A. J. Coleman, Structure of fermion density matrices, Rev. Mod. Phys. **35**, 668 (1963).

[6] J. E. Harriman, Geometry of density matrices. V. Eigenstates, Phys. Rev. A **30**, 19 (1984).

[7] D. A. Mazziotti, Contracted Schrödinger equation: Determining quantum energies and two-particle density matrices without wave functions, Phys. Rev. A **57**, 4219 (1998).

[8] H. Nakatsuji and K. Yasuda, Direct determination of the quantum-mechanical density matrix using the density equation, Phys. Rev. Lett. **76**, 1039 (1996).

[9] F. Colmenero and C. Valdemoro, Approximating q-order reduced density matrices in terms of the lower-order ones. II. Applications, Phys. Rev. A **47**, 979 (1993).

[10] H. Nakatsuji, Equation for the direct determination of the density matrix, Phys. Rev. A **14**, 41 (1976).

[11] D. A. Mazziotti, Approximate solution for electron correlation through the use of Schwinger probes, Chem. Phys. Lett. **289**, 419 (1998).

[12] D. A. Mazziotti, Pursuit of *N*-representability for the contracted Schrödinger equation through density-matrix reconstruction, Phys. Rev. A **60**, 3618 (1999).

[13] J. P. Misiewicz, J. M. Turney, and H. F. Schaefer, III, Reduced density matrix cumulants: The combinatorics of size-consistency and generalized normal ordering, J. Chem. Theory Comput. **16**, 6150 (2020).

[14] J. M. Herbert and J. E. Harriman, Extensivity and the contracted Schrödinger equation, J. Chem. Phys. **117**, 7464 (2002).

[15] S. E. Smart and D. A. Mazziotti, Quantum solver of contracted eigenvalue equations for scalable molecular simulations on quantum computing devices, Phys. Rev. Lett. **126**, 070504 (2021).

[16] S. E. Smart and D. A. Mazziotti, Many-fermion simulation from the contracted quantum eigensolver without fermionic encoding of the wave function, Phys. Rev. A **105**, 062424 (2022).

[17] S. E. Smart, J.-N. Boyn, and D. A. Mazziotti, Resolving correlated states of benzyne with an error-mitigated contracted quantum eigensolver, Phys. Rev. A **105**, 022405 (2022).

[18] S. E. Smart and D. A. Mazziotti, Accelerated convergence of contracted quantum eigensolvers through a quasi-second-order, locally parameterized optimization, J. Chem. Theory Comput. **18**, 5286 (2022).

[19] D. A. Mazziotti, S. E. Smart, and A. R. Mazziotti, Quantum simulation of molecules without fermionic encoding of the wave function, New J. Phys. **23**, 113037 (2021).

[20] D. A. Mazziotti, Exactness of wave functions from two-body exponential transformations in many-body quantum theory, Phys. Rev. A **69**, 012507 (2004).

[21] D. A. Mazziotti, Exact two-body expansion of the many-particle wave function, Phys. Rev. A **102**, 030802(R) (2020).

[22] H. Nakatsuji, Structure of the exact wave function. III. Exponential ansatz, J. Chem. Phys. **115**, 2465 (2001).

[23] D. A. Mazziotti, Anti-Hermitian contracted Schrödinger equation: Direct determination of the two-electron reduced density matrices of many-electron molecules, Phys. Rev. Lett. **97**, 143002 (2006).

[24] D. A. Mazziotti, Anti-Hermitian part of the contracted Schrödinger equation for the direct calculation of two-electron reduced density matrices, Phys. Rev. A **75**, 022505 (2007).

[25] G. Gidofalvi and D. A. Mazziotti, Direct calculation of excited-state electronic energies and two-electron reduced density matrices from the anti-Hermitian contracted Schrödinger equation, Phys. Rev. A **80**, 022507 (2009).

[26] J. J. Foley, A. E. Rothman, and D. A. Mazziotti, Strongly correlated mechanisms of a photoexcited radical reaction from the anti-Hermitian contracted Schrödinger equation, J. Chem. Phys. **134**, 034111 (2011).

[27] J. W. Snyder, Jr., A. E. Rothman, J. J. Foley, IV, and D. A. Mazziotti, Conical intersections in triplet excited states of methylene from the anti-Hermitian contracted Schrödinger equation, J. Chem. Phys. **132**, 154109 (2010).

[28] J. W. Snyder, Jr. and D. A. Mazziotti, Photoexcited conversion of *gauche*-1,3-butadiene to bicyclobutane via a conical intersection: Energies and reduced density matrices from the anti-Hermitian contracted Schrödinger equation, J. Chem. Phys. **135**, 024107 (2011).

[29] A. M. Sand and D. A. Mazziotti, Enhanced computational efficiency in the direct determination of the two-electron reduced density matrix from the anti-Hermitian contracted Schrödinger equation with application to ground and excited states of conjugated π-systems, J. Chem. Phys. **143**, 134110 (2015).

[30] J.-N. Boyn and D. A. Mazziotti, Accurate singlet-triplet gaps in biradicals via the spin averaged anti-Hermitian contracted Schrödinger equation, J. Chem. Phys. **154**, 134103 (2021).

[31] A. Peruzzo, J. McClean, P. Shadbolt, M.-H. Yung, X.-Q. Zhou, P. J. Love, A. Aspuru-Guzik, and J. L. O'Brien, A variational eigenvalue solver on a photonic quantum processor, Nat. Commun. **5**, 4213 (2014).

[32] A. Kandala, A. Mezzacapo, K. Temme, M. Takita, M. Brink, J. M. Chow, and J. M. Gambetta, Hardware-efficient variational quantum eigensolver for small molecules and quantum magnets, Nature (London) **549**, 242 (2017).

[33] J. Tilly, H. Chen, S. Cao, D. Picozzi, K. Setia, Y. Li, E. Grant, L. Wossnig, I. Rungger, G. H. Booth, and J. Tennyson, The variational quantum eigensolver: A review of methods and best practices, Phys. Rep. **986**, 1 (2022).

[34] J. Romero, R. Babbush, J. R. McClean, C. Hempel, P. J. Love, and A. Aspuru-Guzik, Strategies for quantum computing molecular energies using the unitary coupled cluster ansatz, Quantum Sci. Technol. **4**, 014008 (2018).

[35] J. Lee, W. J. Huggins, M. Head-Gordon, and K. B. Whaley, Generalized unitary coupled cluster wave functions for quantum computation, J. Chem. Theory Comput. **15**, 311 (2019).

[36] H. R. Grimsley, S. E. Economou, E. Barnes, and N. J. Mayhall, An adaptive variational algorithm for exact molecular simulations on a quantum computer, Nat. Commun. **10**, 3007 (2018).

[37] X. Liu, A. Angone, R. Shaydulin, I. Safro, Y. Alexeev, and L. Cincio, Layer VQE: A variational approach for combinatorial optimization on noisy quantum computers, IEEE Trans. Quantum Eng. **3**, 1 (2022).

[38] D. A. Mazziotti, Variational method for solving the contracted Schrödinger equation through a projection of the N-particle power method onto the two-particle space, J. Chem. Phys. **116**, 1239 (2002).

[39] A. W. Schlimgen, K. Head-Marsden, L. M. Sager, P. Narang, and D. A. Mazziotti, Quantum simulation of open quantum systems using a unitary decomposition of operators, Phys. Rev. Lett. **127**, 270503 (2021).

[40] M. Motta, C. Sun, A. T. K. Tan, M. J. O'Rourke, E. Ye, A. J. Minnich, F. G. S. L. Brandão, and G. K.-L. Chan, Determining eigenstates and thermal states on a quantum computer using quantum imaginary time evolution, Nat. Phys. **16**, 205 (2020).

[41] A. Daskin and S. Kais, An ancilla-based quantum simulation framework for non-unitary matrices, Quant. Info. Proc. **16**, 33 (2017).

[42] T. Kosugi, Y. Nishiya, H. Nishi, and Y.-I. Matsushita, Imaginary-time evolution by using forward and backward real-time evolution with a single ancilla: First-quantized eigensolver algorithm for quantum chemistry, Phys. Rev. Res. **4**, 033121 (2022).

[43] J. Nocedal and S. J. Wright, *Numerical Optimization*, Springer Series in Operations Research and Financial Engineering (Springer, New York, 2006).

[44] G. Brassard, P. Høyer, M. Mosca, and A. Tapp, in Quantum amplitude amplification and estimation, *Quantum Computation and Quantum Information*, edited by S. J. Lomonaco, Jr., AMS Contemporary Mathematics (American Mathematical Society, Charles Street Providence, Rhode Island, 2002), Vol. 305, pp. 53–74, https://www.ams.org/books/conm/305/.

[45] K. Nakaji, Faster amplitude estimation, Quantum Inf. Comput. **20**, 1109 (2020).

[46] G. E. Crooks, Gradients of parameterized quantum gates using the parameter-shift rule and gate decomposition, arXiv:1905.13311.

[47] J. P. Finley, R. K. Chaudhuri, and K. F. Freed, Applications of multireference perturbation theory to potential energy surfaces by optimal partitioning of H: Intruder states avoidance and convergence enhancement, J. Chem. Phys. **103**, 4990 (1995).

[48] C. A. Schwerdtfeger and D. A. Mazziotti, Low-rank spectral expansions of two electron excitations for the acceleration of quantum chemistry calculations, J. Chem. Phys. **137**, 244103 (2012).

[49] E. P. Hoy and D. A. Mazziotti, Positive semidefinite tensor factorizations of the two-electron integral matrix for low-scaling *ab initio* electronic structure, J. Chem. Phys. **143**, 064103 (2015).

[50] N. C. Rubin, J. Lee, and R. Babbush, Compressing many-body Fermion operators under unitary constraints, J. Chem. Theory Comput. **18**, 1480 (2022).

[51] C. Valdemoro, D. R. Alcoba, L. M. Tel, and E. Pérez-Romero, Some theoretical questions about the G-particle-hole hypervirial equation, Int. J. Quantum Chem. **111**, 245 (2011).

[52] S. J. Smart, S. E. Warren, and D. A. Mazziotti, HCQA – Hybrid quantum computing algorithms for quantum chemistry, https://github.com/damazz/HQCA.

[53] M. S. Anis, A. Mitchell, H. Abraham, A. Offei, R. Agarwal, G. Agliardi, M. Aharoni, V. Ajith, I. Y. Akhalwaya, G. Aleksandrowicz, T. Alexander, M. Amy, S. Anagolum, A.

Gandon, I. F. Araujo, E. Arbel, A. Asfaw, A. Athalye, A. Avkhadiev, C. Azaustre *et al.*, QISKIT: An open-source framework for quantum computing, https://github.com/Qiskit/qiskit/blob/main/CITATION.bib (2021).

[54] IBM QUANTUM, https://docs.quantum.ibm.com/support (2022).

[55] Q. Sun, T. C. Berkelbach, N. S. Blunt, G. H. Booth, S. Guo, Z. Li, J. Liu, J. D. McClain, E. R. Sayfutyarova, S. Sharma, S. Wouters, and G. K.-L. Chan, PySCF: The Python-based simulations of chemistry framework, WIREs Comput. Mol. Sci. **8**, e1340 (2018).